A PRIORI DESIGN OF OPTIMAL ELECTRO-OPTIC MATERIALS FOR LASER EYE PROTECTION

J. Andzelm, A. Rawlett, J. Dougherty
U.S. Army Research Laboratory; AMSRD-ARL-WM-MA
Aberdeen Proving Ground, MD 21005-5069

T.M. Pritchett
U.S. Army Research Laboratory; AMSRD-ARL-SE-EM
2800 Powder Mill Road; Adelphi, MD 20783-1197

C. Rinderspacher, D.N. Beratan, Weitao Yang
Department of Chemistry, Duke University, Durham, NC 27708

G. Lindsay, A. Chafin, M. Davis
Naval Air Weapons Center-WD, China Lake, CA 93555

P. J. Reynolds
Army Research Office, Durham NC 27703

ABSTRACT

The task of protecting soldier eyesight and battlefield optical sensors from potentially damaging effects of high-intensity light has stimulated interest in electro-optic (EO) materials such as EO chromophores inserted into polymeric material. *A priori* design of optimal EO chromophores of Army relevance requires the capability to calculate accurately both the linear absorption properties (in effect, the color) and non-linear optical (NLO) properties of EO chromophores. Here we discuss two major challenges for the computational methods used in EO materials research: 1) efficiency in exploring an extremely large space of possible EO-molecular architectures; and 2) accuracy of calculating ultraviolet-visible (UV-Vis) spectra. We show that the constrained inverse molecular design algorithm (c**IMD**) and the long-range corrected density functional method (**LC-DFT**) facilitate the discovery of new chromophores for Army applications.

1. INTRODUCTION

The development and use of advanced materials in future military systems are critical to attaining performance goals of the Future Force. It is equally important to establish safeguards against pervasive threats by developing protective EO materials. These materials should be transparent in the visible and possess NLO properties characterized by a high value of molecular hyperpolarizability (β) (Pritchett et al.,2008).

This represents a considerable development dilemma, as transparent chromophores are typically small molecules with low EO response. Molecules with the desired large β-values are frequently opaque or, at best, have small windows of visibility, and are, therefore, useless for Army applications. For human eyesight, the optimal UV-Vis absorption spectra of chromophores with large β would be transparent in the 500 to 600 nm range of wavelengths corresponding to a yellow spectral range. This requirement can be achieved if the main absorption peak λ_{max} >> 700nm and the potential second, smaller peak is at λ_{max-1} < 420nm.

In this paper, we investigate two classes of chromophores: 1) tolane- and 2) FTC-based (Fig. 1). The tolane-based chromophores are transparent in the desirable, yellow visible range but have only mid-range β-values. On the other hand, the FTC-based dyes have very large β-values, but absorb strongly in the 500-600 nm range. Figure 1 shows schematically the UV-Vis absorption spectra of these dyes in the visible range. The challenge is to modify the architecture of tolane dyes to increase their β-values without affecting their excellent transparency; while for FTC dyes the primary goal is to enlarge the visibility window in the yellow range.

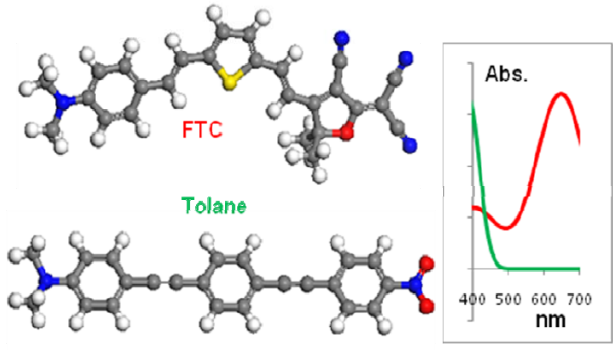

Figure 1. Structure of FTC and tolane and their absorption spectra

The chromophore with phenyl-ethynyl (tolane) motif is presented in Fig. 1. A systematic study of bis(phenylethynyl) benzenes with various donor and acceptor substitutions has been reported (Nguyen et al.,

Report Documentation Page

Form Approved
OMB No. 0704-0188

1. REPORT DATE	2. REPORT TYPE	3. DATES COVERED
DEC 2008	**N/A**	**-**

4. TITLE AND SUBTITLE	5a. CONTRACT NUMBER
A Priori Design Of Optimal Electro-Optic Materials For Laser Eye Protection	5b. GRANT NUMBER
	5c. PROGRAM ELEMENT NUMBER
6. AUTHOR(S)	5d. PROJECT NUMBER
	5e. TASK NUMBER
	5f. WORK UNIT NUMBER
7. PERFORMING ORGANIZATION NAME(S) AND ADDRESS(ES) **U.S. Army Research Laboratory; AMSRD-ARL-WM-MA Aberdeen Proving Ground, MD 21005-5069**	8. PERFORMING ORGANIZATION REPORT NUMBER
9. SPONSORING/MONITORING AGENCY NAME(S) AND ADDRESS(ES)	10. SPONSOR/MONITOR'S ACRONYM(S)
	11. SPONSOR/MONITOR'S REPORT NUMBER(S)

12. DISTRIBUTION/AVAILABILITY STATEMENT
Approved for public release, distribution unlimited

13. SUPPLEMENTARY NOTES
See also ADM002187. Proceedings of the Army Science Conference (26th) Held in Orlando, Florida on 1-4 December 2008, The original document contains color images.

14. ABSTRACT

15. SUBJECT TERMS

16. SECURITY CLASSIFICATION OF:			17. LIMITATION OF ABSTRACT	18. NUMBER OF PAGES	19a. NAME OF RESPONSIBLE PERSON
a. REPORT	b. ABSTRACT	c. THIS PAGE			
unclassified	**unclassified**	**unclassified**	**UU**	**8**	

1997). All the compounds have λ_{max} < 400 nm and the nitro- aminomethyl substitutions possess the largest β of $57x10^{30}$ esu. The 2-dicyanomethylen-3-cuano-4-{2-[E-(4-N,N-di(2-acetoxyethyl)-amino)-phenylene-(3,4-dibutyl) thien-5]-E-vinyl}-5,5-dimethyl-2,5-dihydrofuran (denoted FTC) chromophore were studied extensively, both experimentally (Robinson et al., 1999) and theoretically (Kinnibrugh et al., 2006).

Density functional theory (DFT) is now becoming the most popular method in electronic-structure calculations as it represents a good compromise between computational performance and accuracy. Recently, the performance of various DFT functionals was studied and compared to results of semiempirical (INDO) and Hartree Fock (HF) methods. (Isborn et al., 2007) In that work, molecular structures of several chromophores were optimized by the DFT method followed by a calculation of the molecular hyperpolarizability using semiempirical (INDO), HF and DFT methods, the latter employing various functionals such as B3LYP or PBE. The authors conclude that the relative trends of hyperpolarizability from various computational methods are similar, and therefore consistent use of one method will provide useful guidance for an experimental program.

The visible absorption spectra of chromophores were the subjects of several recent studies prompted by the importance of these organic molecules in the dye industry. Jacquemin et al. (2008) have recently reviewed the performance of various DFT approaches for predicting λ_{max} in the visible region of the electromagnetic spectrum. For some systems, absolute errors as large as 200 nm were reported with a pure DFT method (PBE). The addition of 25% Hartree-Fock exchange as realized in the PBE0-DFT functional improved results considerably. A mean absolute error of 22 nm and a maximum deviation of less than 100 nm were reported for anthraquinone and azobenzene dyes (Jacquemin et al., 2008). Dierksen and Grimme, (2004) found that a significantly larger amount of HF exchange is needed to improve predictions of the absorption spectra for systems with acetylenic bonds.

The deficiencies of DFT in predicting spectra can be associated with the delocalization error of approximate DFT functionals (Cohen et al., 2008). This particularly affects spectra of the push-pull molecules investigated in this work. This error can be partially corrected by including an HF exchange contribution, either constant as stated above, or asymptotically approaching full contribution at long distances between electrons. Long-range-corrected DFT (DFT-LC) was found advantageous in calculations of absorption spectra for some dye molecules. (Jacquemin et al., 2008)

In this paper, we have also used the recently proposed BNL functional (Livshits and Baer, 2007). The BNL functional falls into this DFT-LC class, and it is of particular interest because it has been shown to reproduce exactly the charge-transfer excitation for model systems. Recently, the BNL functional was implemented in the highly parallel NWChem program (Andzelm et al., 2008), and was optimized for several types of chromophores.

Finding optimal architectures of chromophores that may contain numerous substituents in various conformations is a daunting task. The number of accessible compounds with molecular weight below 850 a.m.u. (a typical size of EO chromophores) is staggering at about 10^{200}. More than 20 years of research has established many rules for the optimal design of chromophores, effectively reducing our design space. Nevertheless, surprising new architectures of chromophores are appearing at increased rates with computational chemistry playing an important partnership role in these discoveries. Efficient exploration of enormous molecular spaces requires radically new optimization schemes that search directly for the property optimum, and in the process discover molecular structure.

The typical computational search algorithm parallels the experimental paradigm, by first generating a material structure followed by a calculation of its properties. With luck, sometimes the results are satisfactory. More often than not, we need to continue repeating the search paradigm: **structure → properties**. However, if this paradigm could be inverted into **properties → structure**, we might be able directly to discover a better material with the required properties. In this work we have used the recently proposed inverse molecular design approach (IMD). (Keinan et al., 2007) The IMD methods, utilizing the concept of linear combination of atomic potentials (LCAP) and discrete optimization approaches, allows for the highly-efficient search of optimal properties within millions of possible chromophore architectures.

We have used the recently-developed discrete optimization branch-and-bound/tree-search IMD algorithm (Rinderspacher et al., 2008) to search for the largest hyperpolarizability value in a chemical space of chromophores. In this paper, we have extended this algorithm to perform a constrained IMD search (cIMD) that allows us to find chromophores with large values of β and simultaneously visual clarity. The constraint was introduced via a penalty function algorithm with a soft penalty weight.

In this work, we analyze the properties of tolane molecules and develop new architectures of these dyes

that enhance their β-value while retaining visual transparency. We have also investigated FTC-type chromophores finding substituents that enlarge their visibility window without affecting significant NLO properties of these dyes.

2. METHOD

The chromophores studied in this paper were calculated using either DFT or the semiempirical methods AM1/ZINDO with Gaussian03, NWChem and CNDO software. The structures were fully optimized using the hybrid DFT functional B3LYP with the basis set 6-31G** or the AM1 method. The DFT UV-Vis spectra were predicted from singlet-singlet excitations using the time-dependent density functional theory (TDDFT) method. The semiempirical UV-Vis spectra were calculated using the configuration interaction method with single excitations (CIS) within the semiempirical ZINDO/INDO2 method. The solvation effects were considered using the continuum electrostatic models, PCM and COSMO as implemented in Gaussian03 and NWChem, respectively.

The EO chromophores, sought in this work, should possess a large EO coefficient, which is a function of the first hyperpolarizability (β) and the dipole moment (μ). Therefore, we are interested in maximizing the β_μ value, which is the magnitude of the irreducible part of the β tensor projected on the dipole moment of the chromophore. The β tensor is defined as a nonlinear response to an external electric field. In an electric field, F, the chromophore energy is

$$E(F) = E_0 - \mu^T F - 1/2\ \alpha^T F^2 - 1/3!\ \beta^T F^3 - \ldots$$

where E_0 is the energy in the absence of the electric field, α is the polarizability, and β is the first hyperpolarizability. The hyperpolarizability in the direction of the dipole moment, β_μ , is then calculated as

$$\beta_\mu = (\sum_i \mu_i \sum_j \beta_{ijj}) / |\mu|$$

The static hyperpolarizability β was calculated using a finite-field method.

2.1 LC-DFT calculations

The BNL functional (Livshits and Baer, 2007) based calculations were performed using the NWChem computational chemistry package developed at the Pacific Northwest National Laboratory. This suite of programs has been designed to provide the capability to run large scientific molecular simulations on massively parallel and scalable computers. In the BNL approach, the electron repulsion is separated into long- and short-range parts and given as:

$$\frac{1}{r} = \frac{1}{r} erf(\gamma r) + \frac{1}{r} erfc(\gamma r)$$

where γ is an attenuation parameter. The short-range part is treated with traditional DFT while the long-range component is treated with exact exchange. It can be shown that for large γ the theory becomes more HF-like, while it behaves more pure DFT-like for small γ. We have recently performed an optimization of this parameter for chromophores containing acceptors with tricyano-motif and found that γ = ~0.35 leads to an accurate prediction of absorption spectra with a maximum error of about 30 nm for the most intense absorption peak, λ_{max}. The BNL implementation in the NWChem program results in a highly efficient program to calculate absorption UV-Vis spectra for chromophores of 100 atoms or more (Andzelm et al., 2008)

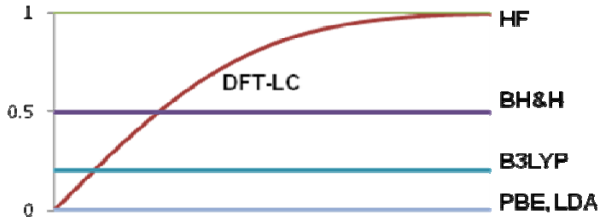

Figure 2. Fraction of HF Exchange vs. inter-electron distance

Figure 2 illustrates the role of exact-HF exchange in various implementations of the DFT methodology. The popular density or gradient-density dependent functionals, LDA or PBE, respectively, do not include any HF exchange and therefore exhibit a large delocalization error. The constant contribution of HF exchange used in B3LYP and BHLYP functionals has a localization error (Cohen et al., 2008) opposite to the delocalization error in LDA. Mixing the two types of functionals causes partial cancellation of errors. The DFT-LC method is effective for this error cancellation at large electron-electron distance and therefore allowing for accurate calculations of absorption spectra.

Table 1 compares the performance of various DFT methods in predicting the absorption spectrum of dyes studied in this paper. For each dye, two main absorption peaks λ_{max} and λ_{max-1} are presented together with oscillator strengths. The experimental oscillator strengths were estimated from absorbance data and normalized to 1.0 for the λ_{max} peak. The 6-31G* basis set was used in DFT and HF calculations for all but BHLYP, where the 6-31+G* basis set was used.

Adding diffuse functions causes a red shift in spectra by up to 20 nm. To compare with experimental data, the solvation effects of chloroform and cyclohexanone were included for the tolane and FTC dye, respectively. The solvent causes a large red shift of the λ_{max} peak by ~90 nm for the FTC dye and a smaller shift of ~60 nm for tolane at the B3LYP/6-31G* level of theory. This is to

be expected because the dipole moment of tolane of 11.6 Debye is much smaller than that of FTC at 22.7 Debye.

Table 1. UV-Vis absorption spectra of dyes from QM calculations. λ_{max} and λ_{max-1} absorption peaks (in nm) and in parentheses oscillator strengths are presented

	Tolane		FTC	
Experiment	384(1.0)	328(0.2)	650(1.0)	400(0.2)
ZINDO	407(1.6)	351(0.1)	568(1.7)	375(0.1)
HF	337(2.4)	230(0.1)	480(2.1)	302(0.2)
LDA	965(0.4)	520(0.9)	811(1.3)	553(0.7)
PBE	918(0.4)	508(1.0)	801(1.3)	550(0.7)
BHLYP	409(2.0)	312(0.6)	573(2.0)	368(0.1)
B3LYP	586(0.7)	404(1.4)	690(1.7)	464(0.5)
M05	520(0.9)	383(1.4)	657(1.7)	440(0.4)
BNL	404(1.6)	265(0.2)	667(1.7)	361(0.2)

The utility of the computational model can be judged by its ability to reproduce both the position and strength of the λ_{max} and λ_{max-1} peaks accurately, thus providing an indication of the width and absorption level in the visible part of the spectrum. Results from Table 1 clearly indicate that both the HF and the DFT methods, without contributions from exact exchange (LDA, PBE) are useless in predicting spectra of dyes. The DFT methods with some HF-exchange contributions (BHLYP, B3LYP, M05) produce erratic results. BHLYP is apparently useful for tolane research, while M05 predicts well the λ_{max} peak of FTC. The DFT-LC methods, such as BNL implemented by us (Andzelm et al., 2008) seem to predict consistently the main spectral features of various dyes.

The λ_{max} peak represents excitations from the highest occupied molecular orbital (HOMO) to the lowest unoccupied molecular orbital (LUMO). This is a charge-transfer excitation because the HOMO is localized on the donor side of chromophores while the LUMO is located on the acceptor side. The significant underestimate of the charge transfer HOMO-LUMO gap in LDA and PBE,

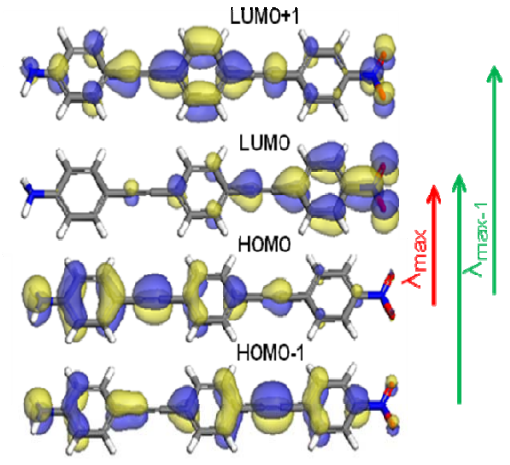

Figure 3. Valence and unoccupied orbitals of tolane

due to the delocalization error (Cohen et al., 2008) is responsible for the underestimate of the excitation energy. The next peak, λ_{max-1}, is due to π- π* excitations, and involves orbitals in close proximity to the HOMO and LUMO levels. Figure 3 shows the valence and unoccupied orbitals of the tolane molecule that dominate the charge-transfer and π- π* excitations.

2.2 cIMD

The inverse molecular design method optimizes molecular property by minimization of its gradient analogue. In our case, the semiempirical method (AM1) is used to obtain geometries and then by changing substitutions in the molecule, the approximate gradient of β is calculated with the ZINOD/S method. Using a discrete analogue of the steepest descent or conjugated gradient algorithm one can find the optimal structure that maximizes β. The key idea that allows for "smoothness" of the property surface allowing application of continuous optimization techniques is the definition of the electrostatic potential $\upsilon(r)$ of a molecule as a linear combination of atomic potentials $\upsilon^R(r)$ (LCAP):

$$\upsilon(r) = \sum_R \theta^R \upsilon^R(r)$$

The θ^R coefficients are continuous variables that define the admixture of an atom (or group of atoms) at position R. This is a smooth embedding of discrete Hamiltonians; analogously, the properties of a discrete set of molecules can be embedded in a smooth space. Given a hierarchy of substitutions, any property of interest can be smoothly interpolated. Each level of a hierarchy of substitutions consists of a list of substitution sites and a set of subsequent levels for each site. Then each element of the set of subsequent levels can be identified with a coefficient from 0 to 1, and the sum over these coefficients for each set must equal 1.

In the following, a systematic method is developed to allow the application of continuous optimization theory to discrete problems. This is achieved by an appropriate embedding of the discrete set of property values P of a library of N molecules. Given an enumeration of this library, where each molecule is associated with a number s and its property value P_s, $\log_2 N$ bits may be used to generate a continuous embedding. For example, assuming the library consists of methane, ethane, propane, and butane, in just that order, then it is possible to interpolate between, e.g., the ground state energies (P=E) of these 4 molecules using two variables, λ_0 and λ_1. The resultant polynomial is just:

$$E(\lambda_0, \lambda_1)=E_0(1-\lambda_0)(1-\lambda_1)+E_1\lambda_0(1-\lambda_1)+E_2(1-\lambda_0)\lambda_1+ E_3\lambda_0\lambda_1$$

As is already obvious from this example, the properties of the polynomial depend on the ordering of molecules. Ordinary interpolation would lead to a

problematic polynomial of degree 3. Generalization leads to the following equations including derivatives, where s' denotes a next neighbor of s at bit j:

$$s=\sum_i 2^i \cdot s(i),\ s(i)\in\{0,1\}, \qquad s'=s+(-1)^{s(j)}\cdot 2^{s(j)}$$

$$P(\{\lambda_i\}_{i=1}^{\log N}) = \sum_{s=0}^{N-1} P_s \prod_{b=1}^{\log N} ((1-\lambda_i)^{s(b)}\lambda_i^{1-s(b)})$$

$$\lambda_i=s(i), \quad \partial P/\partial\lambda_j=(-1)^{s(j)}(P_s-P_{s'})$$

This highly non-linear polynomial in $\log_2 N$ variables with the same order is continuous on $[0, 1]^{\log 2\ N}$ and it allows the adaptation of continuous optimization methods by substituting derivatives *via* simple differences. Since the property in question is left general, a softly weighted penalty function was used to enforce constraints. The following algorithm employed in this work converges due to the local convexity of $P(\{\lambda_i\})$:

1. Start from an initial molecule and mark this molecule as current best.

2. For each substitution site do the following:

(a) For each possible substitution at the current site, attach the substitution and start a conformational search and compute the corresponding β-values. If a constrained optimization is performed the UV-Vis is computed and a penalty is applied to β. The result of the conformation with the lowest energy is recorded for this substitution.

(b) Compute the finite difference derivative and choose the substitution indicated by the largest change in the return values (β for unconstrained optimizations) for its lowest energy conformation. If this is the last substitution site proceed with 3 else continue with 2 at the next site. This is equivalent to choosing the substitution with the largest β for its lowest energy conformation.

3. If the current best molecule matches the last best molecule (structure, energy, property value), exit;

otherwise start over with the current best molecule at step 2.

Unlike branch-and-bound methods, no structures are explicitly excluded from the search space. The overall generality of the algorithm and the interpolation procedure warrant the application of alternative optimization methods including Monte Carlo or genetic algorithms.

This method was tested in predicting the tolane structure with the largest β value as a function of four donor (D) substituents and two acceptor (A) groups shown in Fig. 4. The best, experimentally known, tolane architecture, with D=dimethyl-amine and A=nitro group (Nguyen et al., 1997), is also displayed in Fig. 4. In this test we assume that the donor group can be situated in any position on the L ring, while the acceptor group can occupy any position of the R ring. The total optimization space is then 5*4*5*2=200 molecules. We have performed three runs, starting from three different randomly selected structures. All the runs found the expected structure as shown in Fig. 4, and the longest run finishes in 24 cycles, well below the theoretical maximum of 200.

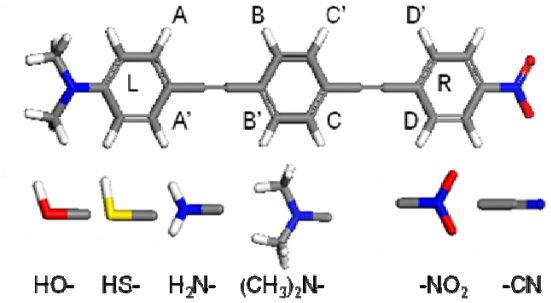

Figure 4. The optimal structure of tolane found by the IMD method

3. RESULTS

Conformations of chromophores are known significantly to affect properties such as the hyperpolarizability, β.(Kinnibrugh et al., 2006) Much less is known on the impact of conformations on the UV-Vis spectra of dyes. One can expect that the NLO properties of tolane dyes will be significantly decreased due to almost free rotations along the single bonds connecting phenyl rings. In this work, we will analyze the effect of tolane bond rotations, and propose attaching substituents in the meta-position of phenyl rings to increase rotational barrier. We will initially study a two-ring tolane (tolane-2), p-amino-p'nitro diphenylethyne.

3.1 Properties of tolane-2

The structure of tolane-2, rotational barriers and relative changes in values of β and λ_{max} as a function of rotational angle along the single bond are presented in

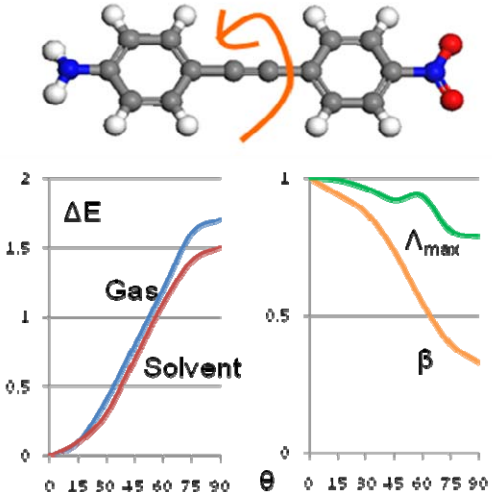

Figure 5. Rotational barrier ΔE (kcal/mol) and relative changes in λ_{max} and β values vs. rotational angle, θ

Fig.5. The maximum barrier at 90 deg is about 1.7 and 1.5 kcal/mol as obtained from gas and solvent (chloroform)–phase calculations at the B3LYP/6-31G** level of the DFT theory. Clearly, any rotamer of tolane-2 can easily be accessed at room temperature. The consequence of almost free rotation is a decrease in the hyperpolarizability (β) value by a factor of 3. The effect of free rotation on the UV-Vis spectra is much less pronounced. The λ_{max} peak of charge-transfer character (384 nm) dominates the spectrum including 60 deg. rotamer. Beginning at 75 deg. the charge-transfer excitation oscillator strength diminishes, and instead the main absorption peak has a π-π character at a much lower absorption of 300 nm. Thus, the rotation of tolane dyes contributes to the significant weakening of NLO properties, and also results in a blue-shift of the absorption spectrum.

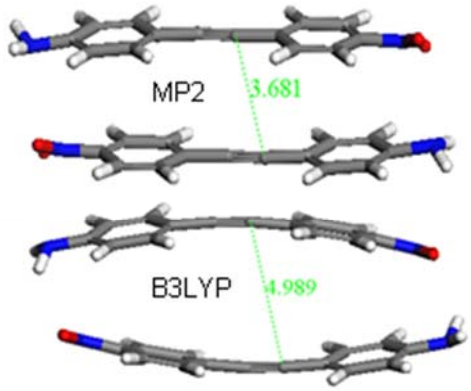

Figure 6. Dimer of tolane-2

Tolane-2 forms stable dimer structures as presented in Figure 6. The B3LYP level of theory, so successful in predicting structures of monomers, fails in calculations for dimmers, because of the lack of dispersion forces in the DFT functional. The MP2 method yields a dimer structure of two planar tolane-2 monomers at a distance of about 3.68 Å measured at the separation between triple bonds on the monomers. The dimer structure is due to the strong electrostatic interactions of two opposite dipole moments of 11.3 Debye each. Due to opposite alignment of dipoles the total moment of the dimer cancels out and the hyperpolarizability becomes negligible. The dimerization of tolane molecules has no effect on the UV-Vis spectra.

This investigation indicates that the NLO properties of tolane-2 can be improved if the free-rotation of phenyl groups around single bonds is blocked and also bulky substituents are attached in order to prevent stacking of tolane monomers.

3.2 Tolane-2 meta-substitutions

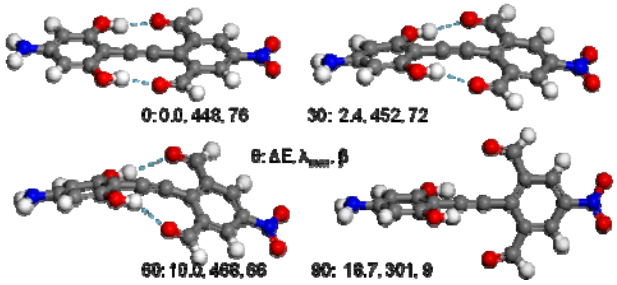

Figure 7. Hydrogen-bonding interactions between hydroxyl and aldehyde groups in meta positions of tolane-2 for rotamers with fixed angle, θ of 0, 30, 60 and 90 deg; ΔE (in kcal/mol), λ_{max}(in nm) and β (in 10^{-30} esu).

Following the conclusions of the preceding section, we have attempted to constrain free rotations around the single bonds by inserting substituents in meta-positions of phenyl rings that strongly interact and raise the barrier for rotation. Figure 7 shows an example of a modified tolane-2 structure with high rotational barrier due to strong hydrogen bonding interaction between the hydroxyl and aldehyde groups. The barrier for rotation (ΔE) is 18.7 kcal/mol. For this rotamer, the main λ_{max} peak of 301 nm has π-π character, and is significantly blue shifted in comparison to the lowest energy rotamer. As expected, the hyperpolarizability is significantly decreased due to the rotation. The pair of substituents -hydroxyl-aldehyde leads to an excellent rotational barrier; however, the main absorption peak of about 450 nm makes this structure too red for our application.

We have examined numerous pairs of substituents searching for structures with low absorption not exceeding 430 nm and with strong hydrogen bonding

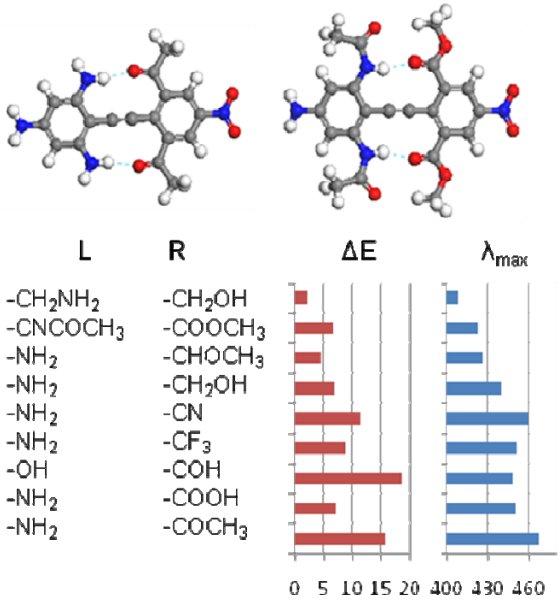

Figure 8. Rotational barriers (ΔE) and λ_{max} for tolane-2 with substituents in meta-positions

stabilizing internal rotations. The results are collected in Figure 8. The amino groups (-NH_2) are strongly bonded to ketone (-$COCH_3$), acid (-COOH) and alcohol (-CH_2OH) substituent groups. The hydroxyl group (-OH) interaction with aldehyde (-COH) and also amine interaction with cyano groups (-CN) also yield significant rotational barriers. Unfortunately, for all these cases the main absorption peak is well above 430 nm indicating an opaque chromophore that is unacceptable for our application. The most transparent chromophores with methylamine-, methoxy-, or amino-ether substituents have rather low rotational barrier. An amido (-$NHCOCH_3$) –ester (-$COOCH_3$) pair was found to produce a rather large barrier to rotation at 7.0 kcal/mol and an acceptable position of the λ_{max} peak at 424 nm.

Figure 8 displays the lowest energy conformers of amine–ketone, and also the amido-ester structures. The rotational barrier can be improved by attaching substituents that form multiple hydrogen bonds resulting in structures with excellent visual properties (λ_{max}= ~400 nm) and significant barriers to rotation of ~17 kcal/mol.

3.3 Tolane-3 meta-substitutions

We have used cIMD method to explore the best substitution sites on tolane-3 that maximize β values and maintain transparency. The optimization space consisted of several substitution groups located in A-D'sites shown in Fig. 4. Our first run (I) included 5 substitutions (-CH_2NH_2, -CH_2OCH_3, -$COOCH_3$, -$NHCOCH_3$, -H) visiting all sites A-D for a total of 5^8 = 390,625 configurations. The second run (II) used a limited number of substitution sites (A, B, C, D) for a total of 5^4=625 configurations. The third run (III) used 9 additional substituents (-NH_2, -CH_3, -OH, -$COCH_3$, -OCH_3, -CF_3, -COH, COOH, -CH_2OH) located at the A, B, C, D sites creating an optimization space of 14^4 = 38,416. The analysis of results was limited to the 20 conformations with largest value of β that also form at least two hydrogen bonds stabilizing rotations around the acetylene-aryl single bonds and have λ_{max} < 420 nm.

We find that amido-ester pairs occur more often in this set of preferable configurations. A small populations of methyloamino-ester and amido-ether pairs was also found. Amide groups were mainly located in meta positions A, A', C and C'. Test number II confirmed that amide-ester pairs at A-B and C-D provide the best β value. Optimization III led to various amine complexes with CF_3 groups that could not be accepted because of the red-shifted spectra.

Inspired by the cIMD simulations, we have built a system based on an amido-ester motif (see Fig 9) for tolane-3 in A-B and C-D positions (Fig. 4) that has excellent transparency λ_{max} = 414 nm and a high value of

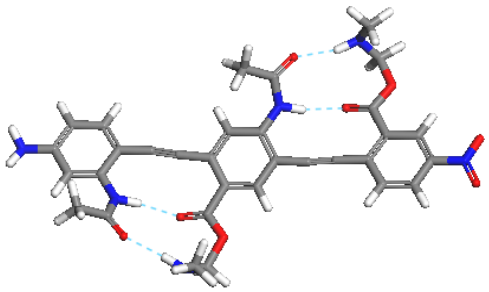

Figure 9. Tolane-3 with amido-ester motif forming multiple hydrogen bonds

β = 225 10^{-30} esu. The double hydrogen bonds between side chains of adjacent phenylene units, stabilize the internal rotation yielding a barrier of 10 kcal/mol. We are currently working on a synthesis of amido-ester functionalized tolane dyes with multiple internal hydrogen bonds. The synthesis of p-phenyleneethynylenes with internal hydrogen bond has been reported. (Hu et al., 2008) However, these are not push-pull type EO molecules of interest in this work (Cross and Davis, 2008), and the synthesis of dyes with the amido-ester motif as shown in Fig. 9 is considerably more challenging.

3.4 FTC substitutions

The FTC chromophore (Fig 1) has several conformers that are close in energy; however, their hyperpolarizabilities vary by as much as 40%. FTC could still be an attractive chromophore for Army applications if not for its poor transparency. The λ_{max}-value is around 650 nm blocking effectively the yellow visibility region of the spectra. In this work we are concerned with designing an FTC architecture that red-shifts the λ_{max} -peak.

The energies of optimized structures, for the lowest six FTC conformers are close, within 2 kcal/mol. We also confirm that the β values may decrease significantly (from 305 to 193 x10^{-30}esu), (Kinnibrugh et al., 2007); however we find that this is not the case for the λ_{max} -peak. The variations in the value of the main absorption peaks are within 15 nm of the λ_{max} for the most stable conformer. We conclude that conformation changes of FTC only slightly affect the UV-Vis absorption spectra.

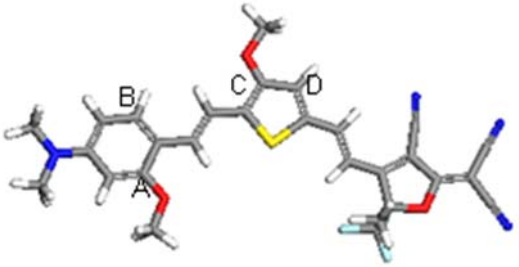

Figure 10. The ethoxy-substituted FTC dye with improved λ_{max}

We performed a cIMD search of the best substitutions in the lowest energy FTC conformer that maximizes the β-value and constrains λ_{max} to be higher than the original value. The search space includes four substitution sites (marked with X=A, B, C, D in Fig 10), choice of donor, and exchanging one of the methyl groups of an acceptor with CF_3. The following groups were considered for the X-sites: hydroxyl, methyl, methoxy, methylthioether, amide, ester and hydrogen. We have also considered amine, methyl-amine and ethyl-amine as donors. The total optimization space contained 14,406 molecules and our search completed in 62 cycles. Analysis of the top 12 structures revealed that the preferable architecture has a CF_3 group at the acceptor site and ethyl-amine as a donor. The best structure shows methoxy substitutions at the A, C and D sites. The A site is predominantly populated with a methoxy group (one occurrence of hydroxyl and amide groups was found). The geometries of these structures were then refined with DFT and calculations of UV-Vis and hyperpolarizability confirmed the findings of the IMD method. The best structure is presented in Figure 10. A significant red-shift of the λ_{max}-peak of about 15% (to 740 nm), and even a slight increase in β-value ($327x10^{-30}$ esu) was found.

CONCLUSIONS

In this work, we have presented a new constrained inverse molecular design algorithm (c**IMD**) and the long-range corrected density functional method (**LC-DFT**). We have shown that these methods facilitate the discovery of new chromophores for Army applications. Specifically, we have found that the self-assembly of hydrogen-bonded substituents in the meta position of tolanes prohibits internal rotations, thus improving significantly the β-value. The amido-ester motif involving multiple intramolecular hydrogen-bonding was found as the best compromise between requirement of achieving high rotational barriers and low UV-Vis absorption. The FTC chromophores were also modified by including CF_3 and methoxy substituents that enlarge the visibility window without affecting the high β-values.

ACKNOWLEDGEMENT

DNB and WY thank the ARO managed DARPA PROM program for support of this project. The authors are indebted to Andrew G. Mott and Robert C. Hoffman for intellectual discussions and insight into this research.

REFERENCES

Andzelm, J., Rawlett, A., Dougherty, J., Govind, N. and Baer, R., 2008: Performance of DFT methods in the calculation of optical spectra of chromophores, *IEEE*, accepted.

Cohen, A.J., Mori-Sanchez, P. and Yang, W.T., 2008: Insights into current limitations of density functional theory, *Science*, **321**(5890) 792-794

Cross, T.A. and Davis, M.C., 2008: Synthesis of Hydroxyalkyl-Substituted, Push-Pull Chromophores based on Diphenylacetylenes, *Synthetic Comm.* **38**, 499-516.

Dierksen, M. and Grimme, S., 2004: A Time-Dependent Density Functional Study on the Influence of Exact Hartree-Fock Exchange, *J. Phys. Chem.* **A108**, 10225-10237.

Hu, W., Zhu, N., Tang, W. and Zhao, D., 2008: Oligo(p-phenyleneethynylene)s with Hydrogen-Bonded Coplanar Conformation, *Organic Lett.* **10**, 2669-2672.

Jacquemin, D.,Perpete, E.A., Scuseria, G.E., Ciofini, I. and Adamo, C., 2008: TD-DFT Performance for the Visible Absorption Spectra of Organic Dyes: Convensional versus Long-Range Hybrids, *J. Chem. Theory Comput.*, **4**, 123-135.

Isborn, C.M., Leclercq, A., Vila, F.D., Dalton, L.R., Bredas, J.L., Eichinger, B.E. and Robinson, B.H., 2007: Comparison of Static First Hyperpolarizabilities Calculated with Various Quantum mechanical Methods, *J. Phys. Chem.* **A111**, 1319-1327.

Keinan, S., Hu, X., Beratan, D.N. and Yang, W., 2007: Designing Molecules with Optimal Properties Using the Linear Combination of Atomic Potentials Approach in an AM1 Semiempirical Framework, *J. Phys. Chem.*, **A111,** 176-181.

Kinnibrugh, T., Bhattacharjee, S., Sullivan, P., Isborn, C., Robinson, B.H. and Eichinger, B.E., 2006: Influence of Isomerization on Nonlinear Optical Properties of Molecules, *J. Phys. Chem*. **B110**, 13512-13522.

Livshits, E. and Baer, R., 2007: A well-tempered density functional theory of electrons in molecules, *J. Phys. Chem. Chem. Phys.* **9**, 2932-2941.

Nguyen, P., Lesley, G., Marder, T.B., Ledoux, I. and Zyss., J., 1997: Second-Order Nonlinear Optical properties of Push-Pull Bis(phenylethynyl) benzenes, *Chem. Mater*. **9**, 406-408.

Pritchett, R.C. Hoffman, R.C., Dougherty, J.M., Orlicki, J.A., Zander, N.E., Andzelm, J., Rawlett, A.M., Davis, M.C., Fallis, S., Chafin, A.P., Lindsay, G.A., Park, D. and Herman, W.N., 2008: *Proceedings of the 2008 Meeting of the Military Sensing Symposium (MSS), Specialty Group on Materials*, paper MC03.

Rinderspacher, B.C., Andzelm, J., Yang, W. and Beratan,D.N., 2008: Discrete Optimization of the Hyperpolarizability of a Chemical Subspace, *to be published*

Robinson, B.H., Dalton, L.R., Harper, A.W., Ren, A., Wang, F., Zhang, Z., Todorova, G., Chen, A.,Steier, W.H., Houbrecht, S., Ledoux, I., Zyss, J. and Jen, AK.Y., 1999: The molecular and supramolecular engineering of polymeric electro-optic materials, *Chem. Phys.*, **245**, 35.